Exp Oncol 2004
26, 2, 118–124

Experimental ONCOLOGY

AUTOFLUORESCENCE OF TRANSPLANTABLE HEPATOMA A22 (MH–A22): PROSPECTS OF TUMOR TISSUE OPTICAL BIOPSY

Mindaugas Tamosiunas[1,], Julija Makaryceva[1], Jurate Labanauskiene[2], Saulius Bagdonas[1], Ceslava Aleksandraviciene[2], Janina Didziapetriene[2], Laima Griciute[2], Ricardas Rotomskis[1,2,*]*

[1]*Vilnius University, Laser Research Center, Vilnius 10222 , Lithuania*

[2]*Institute of Oncology, Vilnius University, Vilnius LT-08660, Lithuania*

***Aim*: Autofluorescence of experimental tumor (hepatoma A22 (MH-A22)) was employed to discriminate the optical differences between necrotic and non-necrotic tumor, hemorrhagic tumor and healthy tissue. *Methods*: The experiment was performed *ex vivo* using the transplantable tumor from the right haunch of hybrid mice (C57Bl/CBA). Blue LED light (λ_{em} = 405 nm) was applied for autofluorescence excitation and fibre optics based spectrofluorimeter was used for spectra detection. *Results:* We observed that necrotic tumor tissue is characterized by the absence of endogenous porphyrins fluorescence, and registered spectra do not possess differences in the red spectral region (600–710 nm) in comparison with normalized autofluorescence spectra of muscle. Moreover, only certain segments of non-necrotic tumor bear the fluorescence of endogenous porphyrins. *Conclusions*: Based on the experimental results, we suggest that the absence of long-waved fluorescence differences between necrotic tumor tissue and healthy tissue, e.g. muscle can impede the demarcation between healthy and tumor tissue. The uneven distribution of endogenous porphyrins in non-necrotic tumor tissue as well as the absence of endogenous porphyrins fluorescence in the small experimental tumors complicates the localization of cancerous tissue based on the autofluorescence registration.**

***Key Words:* autofluorescence, optical biopsy, tumor diagnostics, necrosis, fluorescence imaging, proliferating cell nuclear antigen.**

When the biological tissue is exposed to selected UV or short–wavelength visible light, the fluorescence appears from native chromophores present in the tissue. As reviewed by Richards–Kortum and Sevic–Muraca [1], the major molecules, which contribute to the autofluorescence signal in biological tissue, have been identified as tryptophan (emission at 350 nm), tyrosine (300 nm), phenylalanine (280 nm), chromophores in elastin and collagen (400 nm), pyridoxine metabolites (420 nm), flavins (520–540 nm), nicotinamide adenine dinucleotide (440–450 nm), lipo–pigments (430–460 nm, 540–640 nm) and porphyrins (600–700 nm).

Several studies have been performed to define the potential of autofluorescence for cancer diagnosis. Alfano et al [2] was one the first to observe different spectral profiles of endogenous fluorophores in normal tissues of rat (kidney, prostate) and mouse (bladder) and cancerous tissues. Clinical results, obtained by Yang et al [3] indicated that the fluorescence of endogenous porphyrins could be used for the detection of tumor. The consistency of 89% between autofluorescence and traditional biopsy data was obtained in preliminary diagnosis of buccal carcinoma [3].

Received: March 23, 2004.

*Correspondence: Fax: +37052366006
E–mail: mindaugas.tamosiunas@ff.vu.lt;
ricardas.rotomskis@ff.vu.lt

Abbreviations used: 5–ALA — 5–aminolevulinic acid; CCD — charge coupled device; DAB — 3,3'–diaminobenzidine; FWHM — full width at half maximum; LED — light emitting diode; MVLR — multivariate linear regression analysis; NADH — nicotinamide adenine dinucleotide; PpIX — protoporphyrin IX; PCNA — proliferating cell nuclear antigen.

The origin of endogenous porphyrins appearance in cancerous tissue has been discussed in literature. A. Policard first reported the red fluorescence of necrotic tumors in 1924 (see review [4]). F. Ronchese [5] proposed that ulceration is essential for the production of the red fluorescence in human cutaneous squamous cell carcinoma. Ghadially et al [6] found bright red fluorescence limited to the exterior of ulcerated tumors, and attributed it to endogenous porphyrins. Several possible hypotheses on the protoporphyrin appearance in tumor tissue have been suggested: it is a product derived from microbes; it was produced by the tumor tissue or was taken and accumulated in tumor from the blood stream [7]. The fluorescence of endogenous porphyrins in tumors of oral cavity has been attributed to the presence of several different species of bacteria inhabiting ulcerated and necrotic tissues [8]. Many bacterial organisms that inhabit necrotic tissue are able to produce red fluorescing porphyrins under the presence of exogenous 5–aminolevulinic acid (5–ALA) [9]. Betz et al [10] states that red fluorescence of endogenous porphyrins localizes on the bacterial coating of the necrotic parts of some oral neoplasms after 5–ALA administration.

Supposedly, the enhanced fluorescence of endogenous porphyrins in cancerous tissue (mostly in tumors of non oral cavity) is the consequence of the tumor–specific metabolic alterations [11, 12], results from the porphyrin retention in tumors [13] which can be caused by tumor hypervascularity [14]. The viable part of the brain tumor (astrocytoma) localized in white matter possesses fluorescence peaks assumed to originate from endogenous porphyrins [15]. However, typi–

cal spectra of necrotic tissue of the brain tumor possess no endogenous porphyrin fluorescence. The lowered fluorescence intensity in the blue region of necrotic tumor spectra might be due to the weak fluorescence or reabsorbtion of fluorescent light by blood [15]. The studies of autofluorescence of colorectal cancer demonstrated that endogenous PpIX fluorescence occurred in the absence of necrosis and in sterile locations [12]. PpIX could not be removed from the specimens of colorectal cancer [12] and oral squamous cell carcinoma [11] mechanically indicating that the signal originated from within the tissue. It was proposed, that colorectal cancer metastases accumulate diagnostic levels of endogenous PpIX as a result of alterations in tumor metabolism [12].

Topical or systemic administration of 5–ALA results in selective accumulation of protoporphyrin IX (PpIX) in non–necrotic malignant tissue, most probably due to the deficiency in iron [16] or ferrochetalase [17] in tumor cells. The data on distribution of 5–ALA induced porphyrin in brain tumor (glioma) were presented in [18]. Fluorescence imaging techniques were used to demonstrate that solid non–infiltrating tumor was characterized by strong red fluorescence, whereas infiltrating tumor was generally discernible by less intense, pink fluorescence. Authors [18] point out that tumor necrotic area, which was readily distinguished using normal illumination, did not show significant porphyrin fluorescence in response to 5–ALA application underlining the metabolic nature of porphyrin accumulation in cancerous tissue. It was estimated [19] that excitation with 405 or 436 nm gives poor possibilities to diagnose colon adenoma, when 5–ALA is not applied. The possibility of distinguishing different types of colon tissue was considerably better in patients treated with 5–ALA: sensitivity of 94% (100%) and specificity of 89% (86%) was obtained with 405 nm (436 nm) excitation using multivariate linear regression analysis (MVLR). Authors suggest that there were no apparent advantage in using 5–ALA with 337 nm excitation (the wavelengths of 409, 440, 498, 572, 661 nm were used in MVLR), as autofluorescence provides good discrimination (100% sensitivity and 96% specificity) between normal and adenomatous tissues in colon [19].

Fluorescence spectroscopy is a promising technique for the real time and non–invasive diagnosis of tumors and could fill the gap between the primary examination of tumor and the invasive biopsy. Point spectroscopy, a technique also known as optical biopsy, involves registration of the fluorescence spectrum arising from a single point in tissue. The aim of this study was to examine the autofluorescence spectra of experimental tumor (hepatoma A22 (MH–A22)) and to relate the spectral properties of particular tumor areas to the state of the tissue of malignant tumor. Autofluorescence imaging and the analysis of spectral data collected from cancerous and normal tissues *ex vivo* provide information on the fluorescence properties and distribution of endogenous chromophores in non–homogenous tumors.

MATERIALS AND METHODS

Instrumentation. Autofluorescence measurements were performed with an optical fibre spectrofluorimeter, depicted in Fig. 1. The blue LED light (λ_{ex} = 405 nm) was used for excitation of tissue autofluorescence. A central fibre of bifurcated bundle of 7 fibres (core diameter 200 μm) together with a system of lenses was used to conduct excitation light for continuous illumination of selected tissue sites. Circularly arranged fibres, located at the input end of the fibre bundle, were used to collect tissue autofluorescence. To avoid direct fibre and tissue contact, the input end of the fibre bundle was covered with a glass tip. A 490 nm (T_{490} = 80%) long pass filter was inserted into the detection light path to cut off scattered light of excitation, while allowing autofluorescence to pass through. In order to keep the conditions of fluorophore excitation and detection of fluorescence emission unchanged, all samples were mounted on a stable basement with a micrometric screw. The input end of the fibre was closely fixed above the sample during the measurements. Fluorescence was recorded in 450–800 nm spectral range by means of S2000–FI spectrofluorimeter (Ocean Optics, USA) equipped with a 2048 element linear CCD–array detector and connected to a personal computer.

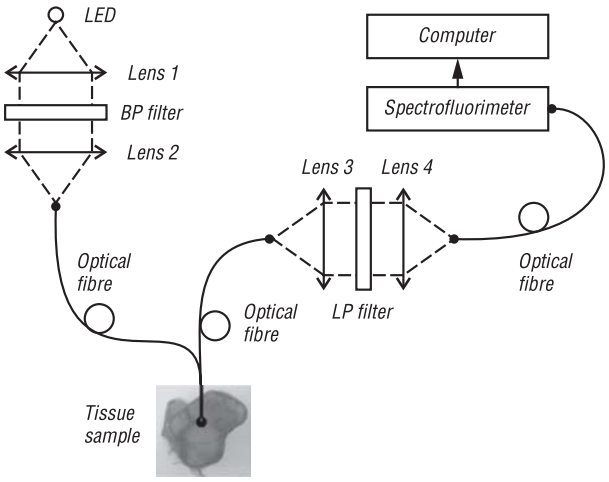

Fig. 1. Schematic diagram of the experimental setup

The fluorescence imaging of tumor tissue was performed using image analysis system (Hamamatsu) equipped with a microscope (Zoom Master, Prior, England), CCD camera (C5405, Hamamatsu, Japan), a RGB monitor (PVM–1454QM, Sony, Japan) and image processor (Argus 20, Hamamatsu, Japan) connected to a personal computer (Fig. 2). A specimen of malignant tissue was placed in a microscope focus plain and autofluorescence profile was registered using an 6W UV light source (T5/BLB, Philips, Holland) for excitation (peak intensity at 365 nm, FWHM = 20 nm) of tissue fluorophores. A 620 nm (T_{620} = 80%) long pass filter was placed before CCD camera in order to record autofluorescence only in the red spectral region.

Tissue samples. An autofluorescence study was performed on 8 hybrid mice (C57Bl/CBA, 8–10 weeks old, female, weight range 21–25 g), obtained from Ani–

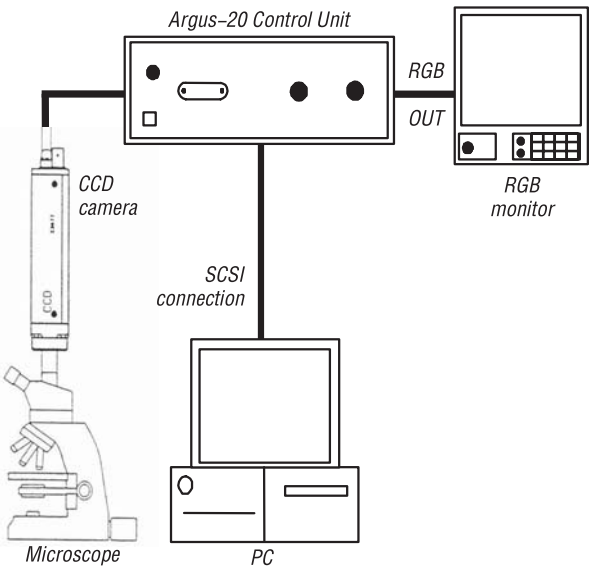

Fig. 2. Block diagram of the image analysis system (Hamamatsu)

mal Facility of Immunology Institute of Lithuanian Academy of Sciences. Hepatoma A22 (MH–A22) was maintained and passaged in Oncology Institute, Vilnius University. Approximately $1 \cdot 10^5$ cells were inoculated subcutaneously to the right haunch of the mice. Tumor growth was documented regularly by measurements with Vernier calliper in three orthogonal dimensions. Experiment started 7 days after inoculation of malignant cells, when the tumor volume reached 0.07 cm^3. Further measurements (6 mice) were performed 9 days, 12 days, 14 days, 16 days and 19 days after inoculation of malignant cells (up to 1 cm^3 of tumor volume). Control specimens of healthy tissue (muscle) were prepared from the same mice. The muscle samples from 2 healthy mice were used for control autofluorescence measurements.

Mice have been sacrificed under the guidelines of Good Laboratory Practice. Tumors were excised from mice and were divided into 2–5 slices (about 3 mm thickness), depending on a size of tumor. Specimens of tumor tissue were placed between two glasses. The delineation of non–necrotic, necrotic and hemorrhagic areas of tumor was performed by microscopy studies on tumor tissue specimens. Point measurements of tumor and muscle autofluorescence as well as imaging of the examined specimens were performed. All specimens were kept on ice during the experiment (up to 4 h after tissue excision).

The expression of the cell proliferation associated marker, proliferating cell nuclear antigen (PCNA), was evaluated by imunohistochemical analysis of the specimens of tumor tissue. The samples of tumor tissue were fixed in 4% neutral formalin for three days, then frozen to – 20 °C and cut with freezing microtome into slices of 4–5 μm width. The imunohistochemical reaction was performed by the method of streptavidyn biotin peroxidation, using the monoclonal antibodies (Mo AK PC10, DAKO AS, Denmark) to reveal the proliferating cell nuclear antigen.

The experiments on animals and animal husbandry were carried out in compliance with national and European regulations and were approved by the Lithuanian Animal Care and Use Committee.

RESULTS

Autofluorescence spectra *ex vivo* were recorded on 22 specimens of tumor tissue and 6 specimens of healthy tissue. The evaluation of tumor morphological structure indicated that the areas of non–necrotic and necrotic tumor are present in specimens of large tumors. Tumor necrosis was not detected in the specimens of the small tumors. Hemorrhagic sites occurred both in tumors and in muscle specimens as a result of tissue resection. We have analysed 90 autofluorescence spectra of non–necrotic areas in tumors, 60 spectra of necrotic tumor areas, 33 spectra of hemorrhagic areas and 25 of healthy tissue (muscle) from tumor–bearing mice. The mean fluorescence spectra of malignant and normal tissues *ex vivo* are presented in Fig. 3. All spectra of cancerous and healthy tissues exhibit broad and poorly structured emission bands in 490–800 nm spectral region under excitation at 405 nm. However, significant spectral modifications were detected depending on the state of tissue.

Autofluorescence spectra of healthy tissue differ from tumor tissue both in spectral shape and intensity. The mean autofluorescence of healthy tissue (muscle) is characterized by the major fluorescence band centered at 560 nm (curve 4, Fig. 3). Autofluorescence of the muscle is more intense comparing to that of tumor tissue; however some muscle spectra exhibit reduced autofluorescence intensity in 490–800 nm spectral region. Spectra of areas of non–necrotic and necrotic tumor tissue (curves 1–3, Fig. 3) are characterised by several bands in 490–710 nm spectral region and lower autofluorescence intensity overall comparing with healthy muscle tissue.

In order to compensate for variation in fluorescence intensity and to distinguish spectral differences, the mean autofluorescence spectra have been normalized to the same intensity at 725 nm (Fig. 4, 5). No additional differences in spectral shape were revealed after normalization of these data to the total integrated area under the spectral curve (data not shown).

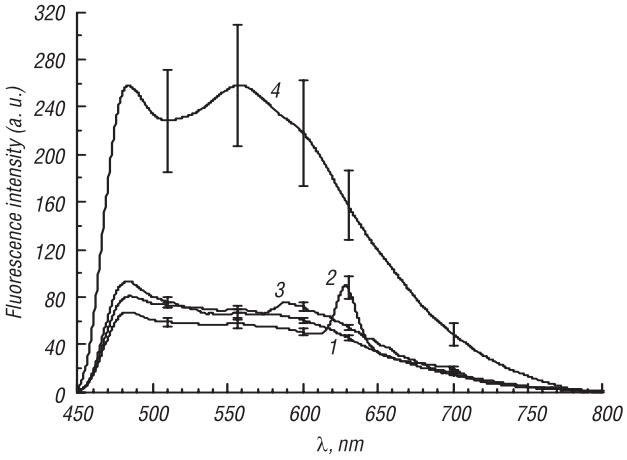

Fig. 3. Mean autofluorescence spectra of healthy and cancerous tissues *ex vivo:* non–necrotic tumor (*1, 2*); necrotic tumor (*3*); healthy tissue (muscle) (*4*)

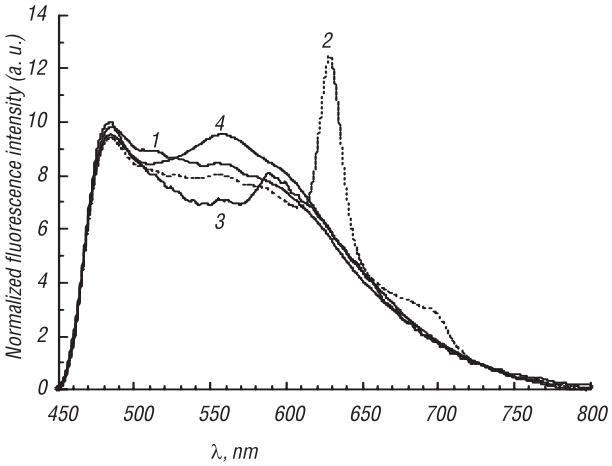

Fig. 4. Mean normalized autofluorescence of healthy and malignant tissues *ex vivo:* non–necrotic tumor (*1, 2*); necrotic tumor (*3*); healthy tissue (muscle) (*4*)

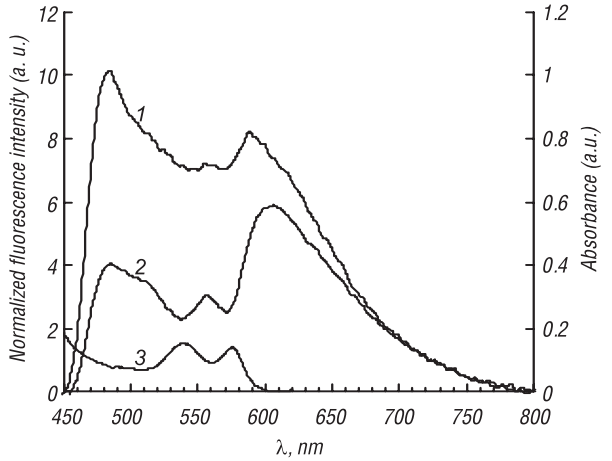

Fig. 5. Effect of blood reabsorbtion on the autofluorescence spectrum: necrotic tumor (*1*), hemorrhagic sites (*2*). Spectrum (*3*) represents blood absorbance

The spectra in Fig. 3 and Fig. 4 (curves 1, 2) indicate that two different spectral types were detected in specimens of non–necrotic tumor. Significant differences in autofluorescence shape occur in 610–710 nm spectral region. A narrow emission band near 633 nm and a broad emission band around 700 nm (spectrum 2 in Fig. 3, 4) are characteristic for limited areas of non–necrotic tumors being measured starting from the 14th day after the inoculation of tumor cells (large tumors). The second type of autofluorescence spectra of non–necrotic tumors (spectrum 1 in Fig. 3, 4) lacked those bands and had similar shape with spectra from necrotic tumor and healthy tissue in 610–710 nm spectral region. Such spectra were detected both in the areas of large non–necrotic tumors and in all tumors being measured up to the 14th day after the inoculation of tumor cells (small tumors).

Distinct variations in shape of spectra from non–necrotic, necrotic and hemorrhagic areas of tumor and also healthy tissue (muscle) occur in 490–600 nm spectral region (Fig. 4, 5). Both types of the mean spectra of non–necrotic tumor exhibit lower relative fluorescence at 560 nm in comparison with muscle fluorescence. The shape of mean autofluorescence spectrum of necrotic tumor tissue (spectrum 3 in Fig. 4, spectrum 1 in Fig. 5) significantly differs from those measured in non–necrotic tumor and muscle in 490–600 nm spectral region. It is characterized by reduced fluorescence intensity in this spectral region with dips around 536 and 577 nm.

Autofluorescence spectra in hemorrhagic areas of tumor tissue, similarly to those of necrotic tumor tissue, are characterized by dips in 500–600 nm spectral region (Fig. 5). The blood absorbance spectrum is presented (Fig. 5, curve 3) for comparative purposes. The absorbtion peaks at 536 and 577 nm belong to hemoglobin.

Additional examination of small and large tumors *ex vivo* was performed using image analysis system equipped with Argus 20 (Hamamatsu) image processor. The morphology of the tumor tissue was preliminary studied under the white light microscope. Microscopy analysis of the large tumor specimens under white light illumination served for the visual delineation of the areas of non–necrotic and necrotic tumor as well as hemorrhagic areas of tumor (Fig. 6, *a*). The white–light images were compared with autofluorescence images obtained under UV light illumination (Fig. 6, *b*). Red autofluorescence was detected only in the areas of non–necrotic tumor when a long band pass filter (T_{620} = 80%) was placed before CCD camera. However, some areas of non–necrotic tumor exhibited no red autofluorescence and by this were undistinguishable from necrotic and hemorrhagic areas of examined tumors. Typical autofluorescence patterns obtained after the imaging of the specimens of small tumors exhibited no red autofluorescence at all (data not shown).

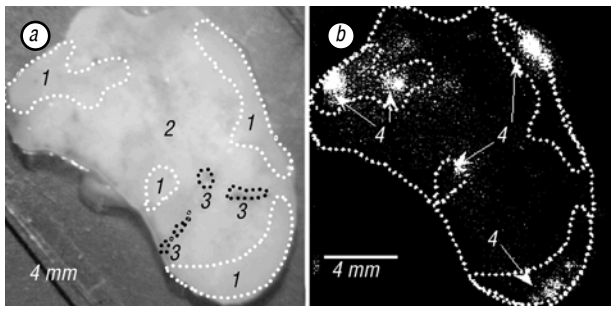

Fig. 6. Typical image of tumor tissue specimen (large tumor) registered under white–light illumination (*a*) and under UV–light excitation (*b*) (see text): (*1*) — non–necrotic tumor, (*2*) — necrotic tumor, (*3*) — hemorrhagic areas, (*4*) — the area of the red fluorescence

The histological analysis of tumor tissue evidenced that the areas of proliferating and necrotic cells naturally occur in the large tumors (Fig. 7). The majority of proliferating tumor cells were distinguished as having an intensive expression of proliferating cell nuclear antigen (PCNA). This expression (up to 98% of positive PCNA$^+$ cells on the average) can be visualized by the product of the chromogenic immunohistochemical reaction (oxidized DAB precipitate) appearing in the cells, which varies in colour intensity (from light brown to dark brown). PCNA negative cells were coloured by hematoxyllyn (light grey/ blue colour), the cytoplasm was stained with 0,1% solution of eosin (from light rose till violet rose colour). The cells of proliferating tumor are enlarged, there are only very small spots of necrosis. The necrotic sites are located near the zones of intense cell proliferation, and

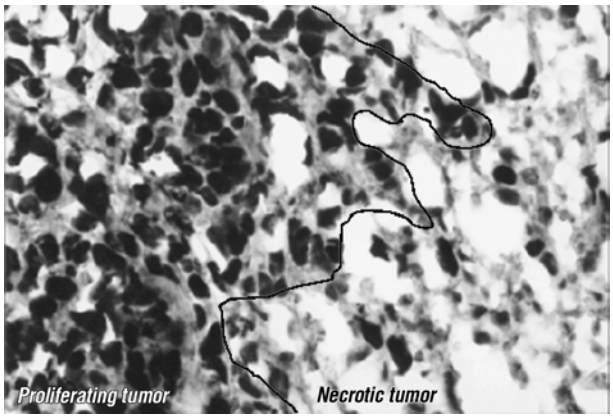

Fig. 7. The histological slides of tumor tissue

the cell density is lower in these sites. The cells pertaining to the karyorrhexis death form (characterized by the absence of nucleus and the presence of many small chromatin fragments) as well as single apoptotic cells and some relict proliferating cells were observed in the area of necrotic tumor.

DISCUSSION

Tissue autofluorescence spectrum contains information about the biochemical composition, the cellular metabolism and the structural matrix of tissue. According to the literature, the major endogenous fluorophores contributing to the measured autofluorescence emission spectra under tissue excitation at 405 nm are flavins, lipopigments, porphyrins and, to a much lesser degree, elastin [1, 4]. The ratio between oxidized and reduced forms of NADH and flavins indicates tissue metabolic activity [20]. Elastin (and collagen) composes the connective tissue, while lipopigments, aromatic amino acids and porphyrins are the end–products of lipid metabolism [1, 4].

In general, our data *ex vivo* are consistent with reports of other authors [15, 21, 22] that tumors differentiate from normal tissues by reduced autofluorescence intensity in 490–600 nm (see Fig. 3). Assuming that biological tissue contains a mixture of many fluorophores, the relative enhancement of autofluorescence intensity in region from 510 to 560 nm (see Fig. 4) in normal tissue could be contributed by lipopigments [23, 24]. While autofluorescence at 520–540 nm spectral region can be attributed to flavins, some authors provide information that fluorescence of flavins in tissue is generally weak [25].

The reabsorption of fluorescence in tumor tissue as a result of increased concentration of hem — based molecules, as well as other spectral differencies between tumors and healthy tissues were reported in [4, 15]. The distortion of autofluorescence spectra in the range of 500–600 nm (Fig. 5, spectrum 2) resembles quite well the inverted bands of blood absorbance. Thus, the dips in autofluorescence spectra of hemorrhagic tissues can be caused by the reabsorption effect due to the presence of hemoglobin, which provides easy identification of the bloodstains on tissue by spectroscopic methods. Autofluorescence spectra of necrotic tumor tissue show resemblance to the spectra measured in bloodstained areas of tumor (Fig. 5, spectrum 1). Diminished autofluorescence of necrotic sites in tumor exhibit the same dips around 542 and 577 nm. This can be explained by the presense of a large amount of blood clots in necrotic tissue. The relative decrease of fluorescence intensity in the middle–waved spectral region theoretically could be employed for the identification of necrotic tumor, although it could be difficult to distinguish between the necrotic tumor tissue and the hemorrhagic (cancerous or healthy) tissue. In such a case, the middle–waved autofluorescence could not provide useful information while performing the spectroscopic examination of tissues in a resection area. In fact, that complicates some aspects of autofluorescence application in diagnostics of malignant tissues especially when it is important to ensure that no malignant tissue is left in contact with healthy tissue after tumor surgery.

The enhanced amounts of endogenous porphyrins naturally occur in some tumors localized e.g. in colon and oral cavity. We state that the optical biopsy of necrotic tumor tissue highlight the absence of the fluorescence bands of endogenous porphyrins (Fig. 3, 4). Our results are in good agreement with results obtained by Anderson–Engels et al [15] showing that autofluorescence of endogenous porphyrins was not detected in necrotic areas of brain tumor. We would like to point out that normalized autofluorescence spectra of necrotic tumor are identical to the normalized spectra of healthy tissue (muscle) in 600–710 nm spectral region. The spectroscopic identification or imaging of the tumor tissue considering only the long–waved autofluorescence becomes inaccurate, as the necrotic places of tumor tissue are spectroscopically attributed to non–cancerous tissue.

The uneven distribution of endogenous porphyrins and significant variations of their fluorescence intensity characterize the autofluorescence of non–necrotic tissue of large tumors (Fig. 4). Our results are in agreement with data reported in [10, 21, 23] that only limited areas of some sections of tumors exhibit fluorescence bands of endogenous porphyrins. Two different types of autofluorescence spectra occur in non–necrotic areas of large tumors (Fig. 4). Type I autofluorescence spectra are characterized by the presence of endogenous porphyrin fluorescence. The fluorescence spectrum with peaks at 633 and 700 nm is interpreted as belonging to endogenous protoporphyrin IX [12]. Type I spectra were obtained in the areas of non – necrotic, non–hemorrhagic tissue of the large tumors, starting from 14th day after the inoculation of tumor cells. Type I spectra were not detected in small tumors. Type II autofluorescence spectra (containing no endogenous PpIX fluorescence bands) were detected in small tumors and in some non–necrotic areas of large tumors. These data imply that the concentration of endogenous porphyrins in tumor tissue (hepatoma A22(MH–A22)) depends on tumor growth rate. When the tumors are small, no endogenous PpIX fluorescence occurs; it can be detected only in the areas of large non–necrotic tumors. The presence of endogenous porphyrins in non–necrotic areas

of the large tumors can possibly be related to the altered metabolism of the cancerous tissue. However, the relationship between the appearance of endogenous porphyrins near the necrotic areas and presense of some porphyrin–producing bacteria in large hepatoma A22 (MH–A22) tumors could not be excluded. Our data state that the measurements of endogenous porphyrin autofluorescence alone are not useful for the detection of hepatoma A22 (MH–A22) tumur, especially at the early growth stage.

Obtained data on fluorescence imaging of tumors are in good agreement with the spectral data. PpIX fluorescence rapidly bleaches within the tissue [15, 26] so the experimental conditions, which minimize the effect of illumination on tumor specimen, were selected. The fluorescence images of specimens of tumor tissue recorded starting from 620 nm revealed an uneven distribution of low intensity autofluorescence, attributed to protoporphyrin IX. To our knowledge, the direct relationship between the enhanced long–waved autofluorescence and microscopic morphology of tissue or cellular structures is not observed [21]. The area of enhanced long–waved autofluorescence does not completely correspond to the area of non–necrotic tumor tissue (Fig. 6, *b*), as some non–necrotic areas of large tumors as well as small tumors (data not shown) were characterized by the absence of endogenous protoporphyrin IX fluorescence. We note that the demarcation line based only on the measurements of endogenous porphyrin autofluorescence intensity can provide misleading data for diagnosis of cancerous tissue: the hemorrhagic and necrotic areas of tumor and some areas of non–necrotic tumor tissues could not be distinguished from a non–malignant tissue by processing the imaging of tumor in the red spectral region.

In conclusion, the present study demonstrates that the shape variations in tumor autofluorescence spectra in 500–710 nm cannot be always related with the state of the tumor tissue.

Our data show that some areas of tumor tissue accumulate higher amounts of endogenous porphyrins, which could be clearly distinguished by red fluorescence, both spectroscopically and by visualization. However, the autofluorescence of endogenous porphyrins alone could not delineate the margins of the tumor. The tumor area possessing enhanced red autofluorescence was found to be smaller than the total area of non–necrotic tissue in tumor specimens. Using 600–710 nm spectral region analysis it was not possible to distinguish early staged hepatoma A22 (MH–A22) tumors from the healthy tissues. Autofluorescence of healthy tissue (muscle) was found to be slightly higher than that of tumor in 550–600 nm spectral region.

Endogenous porphyrins were not detected in necrotic and hemorrhagic areas of the large tumors. Those areas can be distinguished spectroscopically by the decreased green–yellow autofluorescence in 500–600 nm spectral range. However, the similar spectral pattern may characterize the hemorrhagic healthy tissue located near the surgical borders of a tumor.

Thus, the better spectroscopic discrimination between cancerous and healthy tissues can probably be achieved combining autofluorescence data obtained in several spectral regions, particularly, extending the range of fluorescence detection towards the blue spectral region.

ACKNOWLEDGEMENTS

We would like to thank Angele Sukackaite, Rasa Gedminaite and Vladislovas Legenis for the skilled technical assistance. This work was partly supported by Lithuanian State Science and Studies Foundation.

REFERENCES

1. **Richards-Kortum R, Sevick-Muraca E.** Quantative optical spectroscopy for tissue diagnosis. Ann Rev Phys Chem 1996; **47**: 555–606.

2. **Alfano RR, Tata DB, Cordero J, Tomashefsky P, Longo FW, Alfano MA.** Laser induced fluorescence spectroscopy from native cancerous and normal tissue. IEEE J Quant Electron 1984; **20**: 1507–11.

3. **Yang YL, Ye YM, Li FM, Ma PZ.** Characteristic autofluorescence for cancer diagnosis and its origin. Lasers Surg Med 1987; **7**: 528–32.

4. **Wagnières GA, Star WM, Wilson BC.** *In vivo* fluorescence spectroscopy and imaging for oncological applications. Photochem Photobiol 1998; **68**: 603–32.

5. **Ronchese F.** The fluorescence of cancer under the Wood's light. Oral Surg Oral Med Oral Pathol 1954; **7**: 967–71.

6. **Ghadially FN, Neish WJP.** Porphyrin fluorescence of experimentally produced squamous cell carcinoma. Nature 1960; **188**: 1124–224.

7. **Ghadially FN.** Red fluorescence of experimentally induced and human tumours. J Pathol Bacteriol 1960; **80**: 345–51.

8. **Harris DM, Werkhaven J.** Endogenous porphyrin fluorescence in tumors. Lasers Surg Med 1987; **7**: 467–72.

9. **Ghadially FN, Neish WJP, Dawkins HC.** Mechanisms involved in the production of red fluorescence of human and experimental tumours. J Pathol Bacteriol 1963; **85**: 77–92.

10. **Betz CS, Mehlmann M, Rick K, Stepp H, Grevers G, Baumgartner R, Leunig A.** Autofluorescence imaging and spectroscopy of normal and malignant mucosa in patients with head and neck cancer. Lasers Surg Med 1999; **25**: 323–34.

11. **van der Breggen EWJ, Rem AI, Cristian MM, Yang CJ, Calhoun KH, Sterenborg HJCM, Motamedi M.** Spectroscopic detection of oral and skin tissue transformation in a model for squamous cell carcinoma: autofluorescence versus systemic aminolevulinic acid — induced fluorescence. IEEE J Sel Top Quant 1996; **2**: 997–1007.

12. **Moesta KT, Ebert B, Handke T, Nolte D, Nowak C, Haensch WE, Pandey RK, Dougherty TJ, Rinneberg H, Schlag PM.** Protoporphyrin IX occurs naturally in colorectal cancers and their metastases. Cancer Res 2001; **61**: 991–9.

13. **Yang Y, Ye Y, Li F, Li Y, Ma P.** Characteristic autofluorescence for cancer diagnosis and its origin. Lasers Surg Med 1987; **7**: 528–32.

14. **Kusunoki Y, Imamura F, Uda H, Mano M, Horai T.** Early detection of lung cancer with laser-induced fluorescence endoscopy and spectrofluorometry. Chest 2000; **118**: 1776–82.

15. **Andersson-Engels S, Elner A, Johansson J, Karlsson SE, Saliford LG, Stromblad LG, Svanberg K, Svanberg S.** Clinical recording of laser-induced fluorescence spec-

tra for evaluation of tumour demarcation feasibility in selected clinical specialities. Lasers Med Sci 1991; **6**: 415–24.

16. **Rittenhouse-Diakun K, van Leengoed H, Morgan J, Hryhorenko E, Paszkiewicz G, Whitaker JE, Oseroff AR.** The role of transferrin receptor (CD71) in photodynamic therapy of activated and malignant lymphocytes using the heme precursor delta-aminolevulinic acid (ALA). Photochem Photobiol 1995; **61**: 523–8.

17. **el-Sharabasy MM, el-Waseef AM, Hafez MM, Salim SA.** Porphyrin metabolism in some malignant diseases. Br J Cancer 1992; **65**: 409–12.

18. **Stummer W, Baumgartner R.** Fluorescence-guided resection of malignant gliomas utilising 5-ALA-induced porphyrins. Photodynamics News 2000; **3**: 6–7.

19. **Eker C, Montán S, Jaramillo E, Koizumi K, Rubio C, Andersson-Engels S, Svanberg K, Svanberg S, Slezak P.** Clinical spectral characterisation of colonic mucosal lesions using autofluorescence and σ-aminolevulinic acid sensitisation. Gut 1999; **44**: 511–8.

20. **Haringsma J, Tytgat GN.** Fluorescence and autofluorescence. Baillières Best Pract Res Clin Gastroenterol 1999; **13**: 1–10.

21. **Marchesini R, Brambilla M, Pignoli E, Bottiroli G, Croce AC, Fante M, Spinelli P, di Palma S.** Light induced fluorescence spectroscopy of adenomas, adenocarcinomas and non-neoplastic mucosa in human colon. J Photochem Photobiol 1992; **14**: 219–30.

22. **Vo-Dinh T, Panjehpour M, Overholt BF, Farris C, Buckley III FP, Sneed R.** *In vivo* cancer diagnosis of the esophagus using differential normalized fluorescence (DNF) indicies. Lasers Surg Med 1995; **16**: 41–7.

23. **Bottiroli G, Croce AC, Locatelli D, Marchesini R, Pignoli E, Tomatis S, Cuzzoni C, Di Palma S, Dalfante M, Spinelli P.** Natural fluorescence of normal and neoplastic colon: a comprehensive *ex vivo* study. Lasers Surg Med 1995; **16**: 48–60.

24. **Bottiroli G, Croce AC, Locatelli D, Nano R, Giombelli E, Messina A, Benericetti E.** Brain tissue autofluorescence: an aid for intraoperative delineation of tumour resection margins. Cancer Detec Prev 1998; **22**: 330–9.

25. **Schomacker KT, Frisoli JK, Compton CC, Flotte TJ, Richter JM, Nisioka NS, Deutsch TFI.** Ultraviolet laser induced fluorescence of colonic tissue: basic biology and diagnostic potential. Lasers Surg Med 1992; **12**: 63–78.

26. **Robinson DJ, de Bruijn HS, van der Veen N, Stringer MR, Brown SB, Star WM.** Fluorescence photobleaching of ALA-induced protoporphyrin IX during photodynamic therapy of normal hairless mouse skin: the effect of light dose and irradiance and the resulting biological effect. Photochem Photobiol 1998; **67**: 140–9.

АУТОФЛУОРЕСЦЕНЦИЯ ПЕРЕВИВНОЙ ГЕПАТОМЫ А22 (МН–А22): ПЕРСПЕКТИВЫ ОПТИЧЕСКОЙ БИОПСИИ ОПУХОЛЕВОЙ ТКАНИ

***Цель*: аутофлуоресценцию трансплантированной опухоли (гепатома 22 (МН-22)) применили для выявления оптических особенностей опухоли с участками некроза и без таковых, опухоли с участками кровоизлияний и здоровой мышечной ткани. *Методы*: в экспериментах *ex vivo* были использованы ткани опухолей, привитых в правое бедро мышей (C57Bl/CBA). Для возбуждения аутофлуоресценции применяли полупроводниковый диод ($\lambda_{эм}$ = 405 нм). Спектрофотометр, оснащенный волоконно-оптическими световодами, использовали для регистрации спектров аутофлуоресценции исследуемых тканей. *Результаты*: в спектрах некротизированных участков опухоли отсутствуют полосы флуоресценции, характерные для эндогенных порфиринов; в красной области спектра (600–710 нм) не выявлены различия между нормированными спектрами некротизированных участков опухоли и здоровой ткани. Флуоресценция эндогенных порфиринов отсутствовала также в опухолях малого размера и наблюдалась только в некоторых сегментах опухолей большого размера без признаков некроза. *Выводы*: на основе экспериментальных данных мы полагаем, что отсутствие различий в аутофлуоресценции в красной области спектра между некротизированными участками опухоли и здоровой мышечной тканью может обусловливать неточную демаркацию границ опухолевой ткани при проведении оптической биопсии. Неравномерное содержание эндогенных порфиринов в участках опухоли без признаков некроза, а также отсутствие флуоресценции эндогенных порфиринов в опухолях малого размера свидетельствуют о том, что для установления границ опухоли недостаточно руководствоваться одной лишь флуоресценцией эндогенных порфиринов.**

***Ключевые слова*: аутофлуоресценция, оптическая биопсия, онкодиагностика, некроз, флуоресценция, PCNA.**